QUALITATIVE INSIGHTS INTO THE VOLTAGE STABILITY PROBLEM

By

Mohamed Salah Ahmed Mohamed

Abdelrahman A. Karrar
Professor of Electrical Engineering
(Chair)

Ahmed H. Eltom
Professor of Electrical Engineering
(Committee Member)

Gary L. Kobet
Adjunct Professor of Electrical Engineering
(Committee Member)

QUALITATIVE INSIGHTS INTO THE VOLTAGE STABILITY PROBLEM

By

Mohamed Salah Ahmed Mohamed

A Thesis Submitted to the Faculty of the University of
Tennessee at Chattanooga in Partial
Fulfillment of the Requirements of the Degree of
Master of Science: Engineering

The University of Tennessee at Chattanooga
Chattanooga, Tennessee

December 2021

ABSTRACT

This work investigates some of the bus indicators for the problem of voltage stability. The purpose is to learn more about the behavior and to observe the factors that cause mis-ranking in estimating the stability margin.

Three indicators are examined, the L-index, the coupled-port method, and the P-index. it found that the L-index does not have a reliable alarm level, and when flagged with an alarm used for the P-index, it shows a large variation of the estimation accuracy across systems.

Also, the coupled single-port method is a reformulated L-index method with no novelty on estimation, the novelty is only in the presentation.

Finally, the P-index is examined and found to be more reliable if it coincides with a maximum P-index and greater participation in the collapse mode. This is tested on benchmark systems; the results indicate that this approach leads to a better estimation in many cases.

TABLE OF CONTENTS

LIST OF TABLES

LIST OF FIGURES

CHAPTER 1

INTRODUCTION

1.1 Background

Several major blackouts have been linked to voltage collapse in today's highly developed power networks. Voltage collapse has caused millions of dollars in equipment damage and thousands of consumer service disruptions in the past. As a result, tools to monitor voltage stability are being developed to diagnose system conditions and develop preventative actions. Online voltage monitoring systems can help predict voltage collapse and rectify problems before they become serious. However, it remains a difficult challenge to estimate the collapse point precisely in an actionable period.

1.2 Problem Statement

In the literature, a number of different approaches for assessing voltage stability have been presented [1]. They are all aimed at estimating the likelihood of a collapse. However, several drawbacks have been identified in relation to these techniques. Some of them display nonlinear behavior as a result of discontinuities introduced by system controls. Many of the others are computationally costly, making them unsuitable for use in online-based applications. Some are unreliable and only operate in specific circumstances. In certain cases, it has even been proven that they have a faulty theoretical foundation.

1.3 Objective

The main purpose of this work is to study a few bus indicators for the problem of voltage stability, particularly three indicators, the L-index, coupled-port method, and the P-index. Observing the behavior and factors that could lead to incorrect ranking and significant errors in stability margin estimation is the target.

1.4 Thesis Layout

The remainder of the thesis is structured as follows:

- Chapter 2: This chapter provides an overview of the literature on various voltage stability analysis tools.
- Chapter 3: In this chapter, we examine more closely three bus indicators, the L-index, the coupled-single port method, and the P-index.
- Chapter 4: this chapter presents simulation results when applying the examined methods on different test systems. Moreover, a discussion on the performance of the proposed method is presented.
- Chapter 5: This chapter concludes the contributions and findings of this work. Furthermore, it provides suggestions and recommendations for future research work.

CHAPTER 2

LITERATURE REVIEW

2.1 Introduction

At any point in time, a power system operating condition should be stable, meeting various operational criteria, and it should also be secure in the event of any credible contingency. Voltage stability, as defined by the IEEE/CIGRE Task Force, is the ability of a power system to maintain steady voltages across all buses after being subjected to a disturbance from a given initial operating condition [2]. Voltage stability incidents might last from a few cycles to many minutes. Voltage stability may be categorized into two types based on their time spans: transient voltage stability and long-term voltage stability. Transient voltage stability occurs between zero and 10 seconds, but long-term voltage stability frequently occurs across many minutes.

Voltage instability is affected by three major factors: load dynamics, generation, and transmission system limits.

- Load dynamics: When the load dynamics are attempting to restore power demand above the transmission network's capacity and the connected generation, voltage instability occurs. When the voltage starts to drop after a disturbance, constant power loads such as industrial motor loads, air conditioners … etc. tend to maintain their active power consumption through the action of motor slip adjustment, distribution voltage regulators, thermostats … etc.

- Generation limits: In the event of a disturbance, if any of the generators exceed their field or armature current time-overload capability limitations, the system voltage will be weak in reactive power.
- Transmission system limits: transmission lines with significant inductance contribute to voltage instability. The voltage drop makes it difficult to transmit electricity or support voltage on the transmission line. If the load is too heavy or the generation is too far from the load centers, the power transfer and voltage support are even more constrained.

The IEEE/CIGRE joint task group on stability defines voltage collapse as "the process by which the sequence of events accompanying voltage instability leads to a blackout or unacceptable low voltage profile in a significant part of the power system" [2]. Voltage collapse is a system instability that can affect several components or the entire system, causing a "blackout". It happens in heavily loaded systems. Voltage instability is caused by insufficient reactive power supplies when the system cannot satisfy demand. As the load increases, voltage drops until voltage-sensitive protection devices come in, causing uncontrollable outages. These outages might lead to a total blackout. Several blackouts across the world have been caused by voltage instability and voltage collapse. For example, New York 1970, France 1978 and 1987, Northern Belgium 1982, Tokyo 1987…etc.

2.2 P-V and Q-V Analysis

A P-V curve plots the power injection against the related voltage change at a particular bus. Figure 2.1 shows a P-V curve. The stable region is located in the upper portion of the curve (above the horizontal dashed line), while the unstable region is at the bottom (below the horizontal dashed

line). The stability limit is the tip of the nose curve. This information is collected via continuous power flow. The Jacobian matrix of power flow equations becomes unique at the voltage stability limit, and therefore the normal power flow solution cannot converge. By reformulating the load-flow equations, the continuing power flow can maintain good conditioning under all loading circumstances. Load-flow equations for stable and unstable equilibrium points can be resolved using this (that is, for both upper and lower portions of the V-P curve).

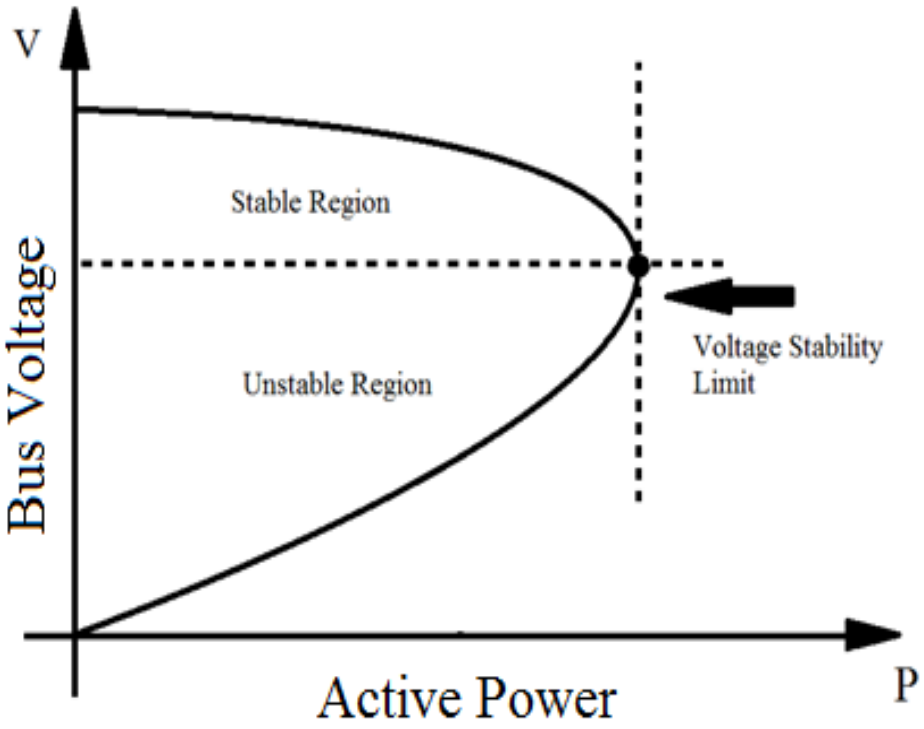

Figure 2.1

Active power loading relationship with bus voltage (P-V curve) [3]

V-Q curves are also helpful in understanding voltage stability. These curves show the sensitivity and variation of bus voltages with respect to reactive power injections. Figure 2.2 shows a V-Q

graph. At the point when dQ/dV = 0, the voltage stability limit is located at the bottom of the curve. A Q increase is paired with a V increase on the right side of the curve. When a rise in Q indicates a drop in V, system is unstable (left side of the curve).

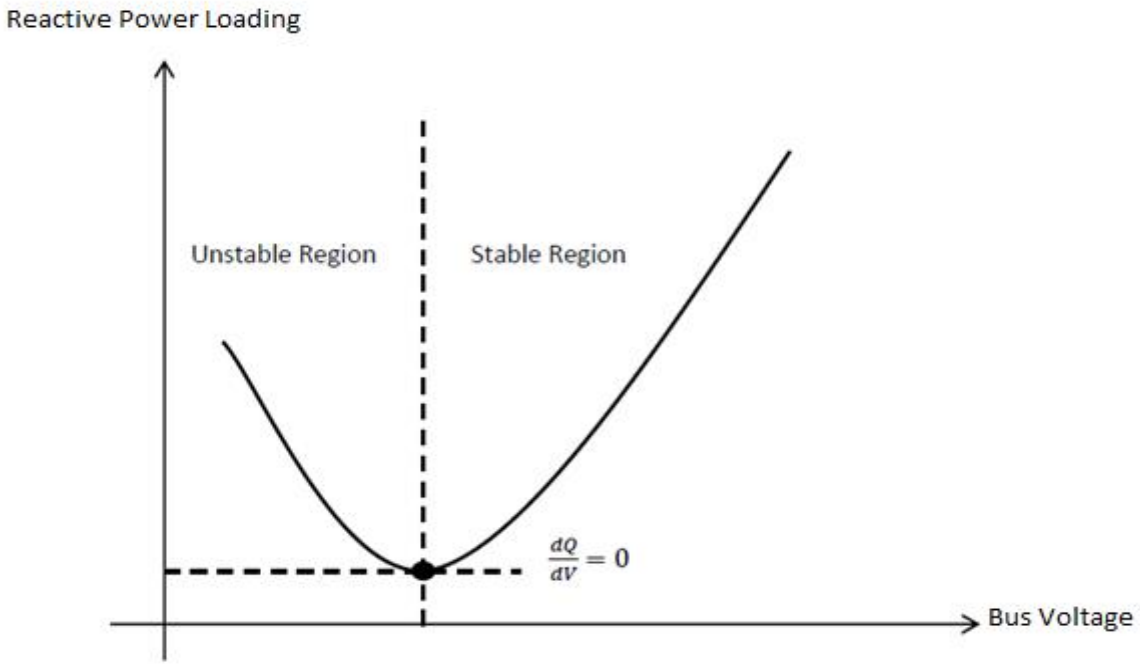

Figure 2.2

Reactive Power Injection and Bus Voltage Relationship Curve (V-Q) [3]

P-V and V-Q curves are one of the most considered methods to find active power margin and reactive power margin. The major drawback of these curves is, however, that a significant number of these curves would need to be provided with comprehensive information on the voltage stability of the entire system for many various operating points and contingencies. The execution of a huge number of power flows produces each of these curves. This makes the monitoring of the stability of large power systems online highly time-consuming and thus not practicable.

2.3 Continuation Power Flow

As previously mentioned, the Jacobian matrix used for conventional power flow analysis at the moment of collapse becomes singular. This issue may be fixed by using continuation power flow techniques, which reformulate load flow equations to keep the P-V nose curve in a well-conditioned state at all operating circumstances. The two steps of the power flow (PF) process are called the predictor and the corrector [2]. As shown in Figure 2.3, a tangent predictor is used to estimate solution B from the known starting solution A for a given increase in load. Using conventional load flow analysis, the corrector will then find solution C, with the same system load as used in B. To provide even more accurate predictions, a new tangent predictor is then employed. If the maximum point is exceeded, a corrector step with a fixed load will not converge. When this scenario occurs, a corrective step with a constant voltage is utilized to solve the problem.

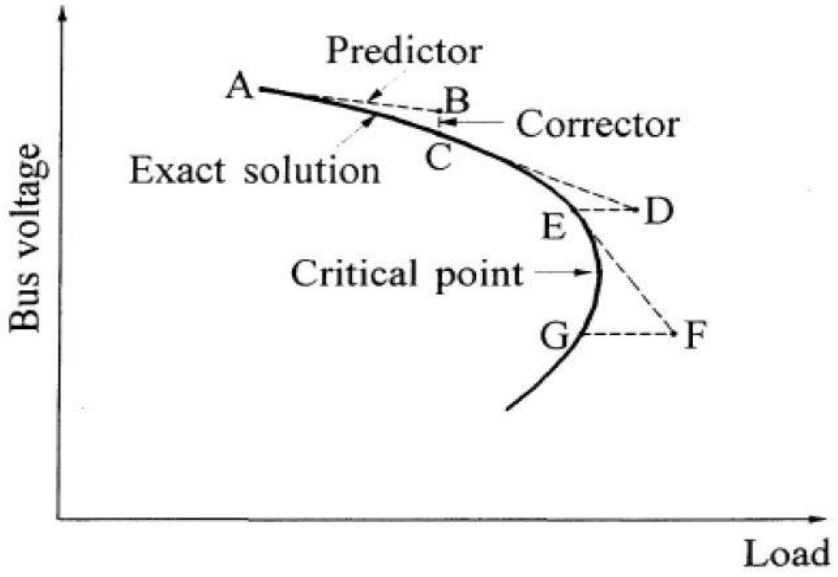

Figure 2.3

Continuation Power Flow Predictor-Corrector Scheme

2.3.1 Mathematical formulation

Similar to conventional load flow, power continuation flow equations are expected to include an additional component that indicates a load increase. This is as follows:

$$F(\theta, V, \lambda) = 0 \tag{2.1}$$

Where:

V is the vector of bus voltage magnitudes.

θ is the vector of bus voltage angles.

λ is the loading parameter.

2.3.1.1 Predictor step

In this step, the next solution for a change in one of the variables θ, V, or λ is estimated using a linear approximation of equation (2.1). Equation 2.1's first derivative is used to generate the following set of linear equations.

$$F_\theta d\theta + F_v dV + F_\lambda d\lambda = 0 \tag{2.2}$$

$$[F_\theta \quad F_v \quad F_\lambda] \begin{bmatrix} d\theta \\ dV \\ d\lambda \end{bmatrix} = 0 \tag{2.3}$$

A new equation is to be introduced to this set to make up for the addition of the loading parameter λ. This is done by setting one of the components of the tangent vector to -1 or +1. This component is called the continuation parameter.

$$\begin{bmatrix} F_\theta & F_v & F_\lambda \\ & e_k & \end{bmatrix} \begin{bmatrix} d\theta \\ dV \\ d\lambda \end{bmatrix} = \begin{bmatrix} 0 \\ \pm 1 \end{bmatrix} \tag{2.4}$$

Where e_k is a row vector with all elements equal to zero except for that corresponding to the continuation parameter which is set to 1.

Initially, the loading parameter λ is set as continuation parameter. The state variable that suffers the largest rate of change near the supplied solution is, nevertheless, modified throughout future predictor stages. If the slope of that parameter moves in one direction, the tangent vector will have the opposite sign. In terms of the limits of the voltage being increased, it is important to point out that the variable with the highest rate of change is often a voltage. One way to find the value of the next solution for equation 2.4 is to do the following:

$$\begin{bmatrix}\theta\\V\\\lambda\end{bmatrix} = \begin{bmatrix}\theta_0\\V_0\\\lambda_0\end{bmatrix} + \sigma\begin{bmatrix}d\theta\\dV\\d\lambda\end{bmatrix} \tag{2.5}$$

The step σ is selected so that a load flow solution exists with the specified continuation parameter. In the event that the corrector step does not find a solution, σ must be decreased and a corrector step repeated until a solution is found.

2.3.1.2 Corrector step

Equations to be solved in this step is:

$$\begin{bmatrix}F(\theta, V, \lambda)\\x_k - \eta\end{bmatrix} = [0] \tag{2.6}$$

Where x_k represents the chosen continuation parameter and η is its predicted value. This set of equations can be solved using the Newton-Raphson method. It should be observed that the introduction of the new x_k equation makes the Jacobian matrix at loading limit non-singular, allowing further analysis beyond the loading limit to get solutions for the lower portion of the P-V nose curve. The symbol of $d\lambda$ indicates if the load limit has been reached. Before the collapse point, this sign is positive, but it becomes negative after that. If the continuation parameter is set

to λ, the corrector step is a vertical line. In contrast, the corrector step is horizontal if a voltage is chosen to represent this parameter.

The continuation power flow is said to be costly in terms of calculation time, despite its robustness and flexibility in handling problems caused by the difficulty of convergence. it is important to use both conventional load flow methods and continuation methods together in order to speed up the solution process. Conventional load flow methods are applied when starting from the base case. The continuation approach is used only when load flow approaches are running into the load limit. Although many modified continuous power flow techniques have been proposed in the literature, nevertheless it is important to point out that several of them have also undergone substantial modifications. These algorithms provide various methods for choosing the step size or method for adjusting the control loop setting. However, all of these plans are built upon the same plan outlined here.

2.4 Voltage stability indices

In the literature, a large variety of voltage stability monitoring and assessment indicators have been proposed. A voltage stability index is a scalar magnitude that can be tracked as system parameters fluctuate [4]. These indices can explain the two voltage instability fundamental aspects defined in [2]: proximity to voltage collapse, i.e. how close the system is to voltage instability, and the process of voltage instability by highlighting the system's weak points. Voltage stability indices (VSIs) are divided into two types: Jacobian matrix-based VSIs and system variables-based VSIs. Using a Jacobian matrix for voltage stability indicators (VSIs) is useful for computing the voltage collapse point and determining the voltage stability margin. Although Jacobian matrix-based VSIs have many advantages, the major issue is their high computation time. Due to this, they are not

suited for voltage instability assessment in an online context. On the other hand, system variables-based VSIs have the admittance matrix elements, and some system variables, such as line voltages or power flow. These indices take less time to compute than Jacobian matrix-based VSIs, making them more suitable for online monitoring. The fundamental drawback of these indices is their inability to precisely estimate the margin. They are, nevertheless, capable of identifying critical buses and lines.

2.4.1 Jacobian matrix-based VSI

When the voltage collapses, the minimum magnitude of the power flow Jacobian matrix's eigenvalues is zero. An index of voltage stability based on the Jacobian matrix's minimum singular value was developed in [5]. Because of the non-linear behavior towards the stability limit, this index was unable to accurately estimate the voltage collapse point[4]. Researches tried to avoid this non-linearity problem, and new power flow Jacobian matrix-based indices were proposed such as:

- V/V0 ratio [6], which is the ratio between the bus voltage V (known from load flow or state estimation studies) and V0, obtained by calculating load flow for the system in the same state but with no loads. This ratio is determined at each system node, allowing for the diagnosis of weak spots.
- Test Function [7], this function predicts the point at which the voltage will collapse using a quadratic modeling approach.
- Tangent Vector [8], shows how varying the load multiplier λ affects system variables (such as bus voltage magnitudes and angles).
- Second Order Index [9] or index I.

2.4.2 System variables-based VSI

The other group of voltage stability indices is based on measurements made directly in the power system, such as bus voltages and admittance matrix components. These indices are useful for online monitoring and assessing voltage instability since they demand less computing cost. The system variables-based VSIs are classified into two groups: line stability indices and bus voltage computation indices (or nodal voltage stability indices)[4].

Power transmission concepts on single lines are the basis of most line stability indicators. In addition to the Lmn index [10], there are several other useful indices, such as the Line Voltage Stability Index (LVSI) [11], LQP-index [12], the Fast Voltage Stability Index (FVSI) [13], and the Voltage Collapse Point Indicators (VCPI) [14].

2.4.2.1 The L index

The L index is a voltage stability indicator that predicts voltage instability or voltage collapse based on information from a normal load flow. It has a value between 0 (no-load system) and 1 (voltage collapse) [15].

According to the L index, the transmission system is represented by a hybrid (H) matrix, which has the following set of equations:

$$\begin{bmatrix} V_L \\ I_G \end{bmatrix} = [H] \begin{bmatrix} I_L \\ V_G \end{bmatrix} = \begin{bmatrix} Z_{LL} & F_{LG} \\ K_{GL} & Y_{GG} \end{bmatrix} \begin{bmatrix} I_L \\ V_G \end{bmatrix} \quad (2.7)$$

Where:

V_L, I_L = Vectors of voltages and currents at consumer nodes.

V_G, I_G = Vectors of voltages and currents at generator nodes.

$Z_{LL}, F_{LG}, K_{GL}, Y_{GG}$ = submatrices of the H-matrix.

Using a partial inversion of the admittance matrix (Y), the H matrix can be derived by changing voltages at consumer nodes against consumer node currents.

The L index is defined as follows for any load node j using the above representation:

$$L_j = \left| 1 + \frac{\underline{V}_{0j}}{\underline{V}_j} \right| \tag{2.8}$$

Where:

$$\underline{V}_j = \sum_{i \in L} \underline{Z}_{ji} \cdot \underline{I}_i + \sum_{i \in G} \underline{F}_{ji} \cdot \underline{V}_i \tag{2.9}$$

And:

$$\underline{V}_{0j} = - \sum_{i \in G} \underline{F}_{ji} \cdot \underline{V}_i \tag{2.10}$$

A consumer bus's L index increases in response to increasing load until it hits 1 at voltage collapse. Hence, buses with higher L index are the weakest.

To explain why the L index is equal to 1.0 at power transfer limit, Equation (2.8) may be written as:

$$L_j = \left| \frac{\underline{V}_j + \underline{V}_{0j}}{\underline{V}_j} \right| \tag{2.11}$$

Then, substituting for $\underline{V}_j$ and $\underline{V}_{0j}$ in the numerator from equation (2.9) and equation (2.10):

$$L_j = \left| \frac{\sum_{i \in L} \underline{Z}_{ji} \cdot \underline{I}_i}{\underline{V}_j} \right| \tag{2.12}$$

This means that the L index is essentially the magnitude of the ratio of the voltage drop along the line to the bus voltage. At maximum power transfer, the voltage drop is equal to bus voltage, and the ratio achieves a magnitude of 1.0.

Using the analogy of a two-bus system, the L index is extended to an n-bus system. With an increase in the number of buses, this leads to inaccurate estimations [16].

2.4.2.2 Concept of coupled single-port circuit

According to the authors of the Coupled-Single-Port Circuit [17], the basic flaws in the application of the single-port Z-match technique to power systems are the inclusion of all other loads in the equivalency of the system. These are nonlinear and dynamic loads. Even if their power levels are consistent, it is theoretically impossible to express them as a single value. One possible solution is to keep all loads outside the equivalent system as indicated in Figure 2.4.

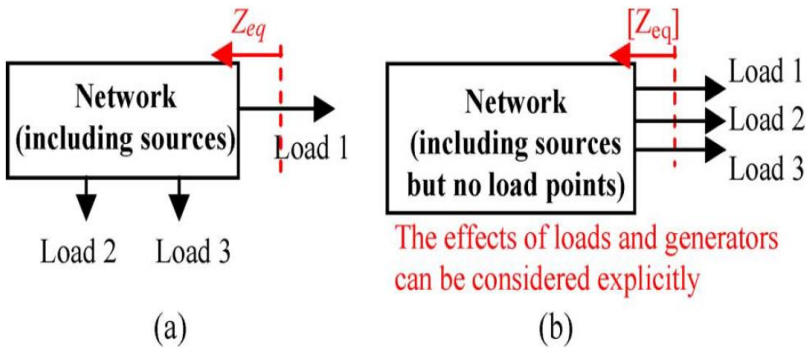

Figure 2.4

Single-port equivalent versus multi-port network equivalent. (a) Single-port equivalent system. (b) Multi-port network equivalent [17]

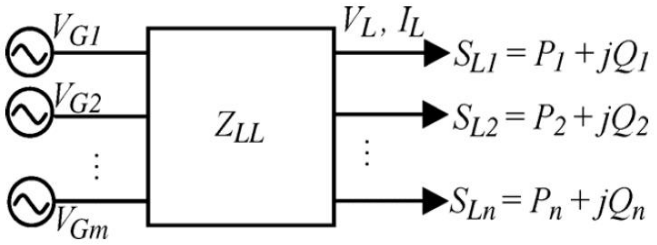

.

Figure 2.5

Multi-port network system model [17]

Again, according to the authors, this problem needs to be addressed. This results in the idea of the equivalent multi-port network. As illustrated in Figure 2.5, the multi-port network is modeled. All generators and load buses are removed from the system. The transmission network is transformed into a matrix of impedance. Then, the multi-port power system can be described by

$$\begin{bmatrix} -I_L \\ 0 \\ I_G \end{bmatrix} = [Y] \begin{bmatrix} V_L \\ V_T \\ V_G \end{bmatrix} = \begin{bmatrix} Y_{LL} & Y_{LT} & Y_{LG} \\ Y_{TL} & Y_{TT} & Y_{TG} \\ Y_{GL} & Y_{GT} & Y_{GG} \end{bmatrix} \begin{bmatrix} V_L \\ V_T \\ V_G \end{bmatrix} \tag{2.13}$$

Where the Y matrix is known as the system admission matrix, V and I indicate voltage and current vectors, and L,T, and the G, respectively, represent load bus, tie bus, and generator bus. Eliminate the tie buses, and the above equation can be expressed as follows:

$$V_L = KV_G - Z_{LL}I_L \tag{2.14}$$

$$Z_{LL} = (Y_{LL} - Y_{LT}Y_{TT}^{-1}Y_{TL})^{-1} \tag{2.15}$$

$$K = Z_{LL}(Y_{LT}Y_{TT}^{-1}Y_{TG} - Y_{LG}) \tag{2.16}$$

where K is an $n \times m$ matrix obtained from system admittance matrix Y , and Z_{LL} is an $n \times n$ impedance matrix. From the above equations, for load bus, it can obtained:

$$V_{Lj} = E_{eqj} - Z_{eqj}I_{Lj} - E_{coupled-j} \tag{2.17}$$

Where:

$$Z_{eqj} = Z_{LLjj} \tag{2.18}$$

and,

$$E_{eqj} = [KV_G]_j \tag{2.19}$$

$$E_{coupled-j} = \sum_{i \neq j; i=1}^{n_L} Z_{LLji} I_{Li} \tag{2.20}$$

Where Z_{eqj} is the Thévenin impedance of the network at bus j, again without the other loads. As can be observed, the diagonal element of the impedance matrix is equal to the bus short-circuit impedance. As long as the topology of the system does not change, it is a constant. $E_{coupled-j}$ indicates the effect of other loads on the bus, which is referred to as the coupling effect in this study.

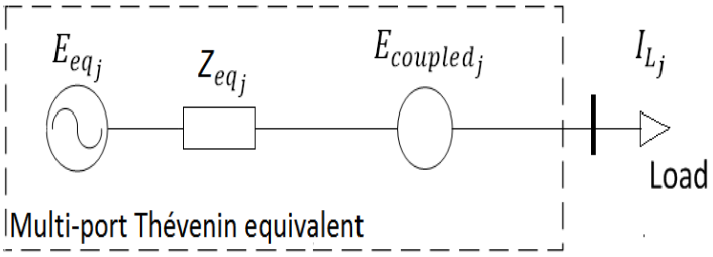

Figure 2.6

Coupled single-port system equivalent

The circuit corresponding to equation (2.20) is shown in Figure 2.6. This is a single-port network and it can be applied to all load buses. In comparison to the previous single-port equivalent circuit, the new term $E_{coupled-j}$ represents the impact of other loads on the bus's equivalent circuit, which is different. This approach can be used to break down a power system into a series of single-port circuits that explicitly include the impact of other loads. This study refers to the new equivalent circuit as a "coupled single-port circuit."

Maximum power that can be delivered to the measurement point can be calculated using matching impedance condition $|Z_{load}| = |Z_{eq}|$ which gives:

$$S_{max} = \frac{\left|E_{eq}^2\right|\left|Z_{eq}\right| - \left(imag\left(Z_{eq}\right)sin\delta + real\left(Z_{eq}\right)cos\delta\right)}{2\left[imag\left(Z_{eq}\right)\,cos\delta - real\left(Z_{eq}\right)\,sin\delta\right]^2} \tag{2.21}$$

$$margin_n = \frac{S_{max,n} - S_{Ln}}{S_{Ln}} \times 100\% \tag{2.22}$$

where S_{max} is the maximum apparent power at the study bus, δ represent the power factor angle of the load, and S_{Ln} is the apparent power of the load at the base case.

2.4.2.3 The P-index

A new voltage stability indicator called P index was developed to quantify proximity to voltage collapse for online assessment of the system voltage stability [16]. The P index can also be used to determine which buses in a system are the weakest. A 0 indicates no-load, whereas a 1.0 indicates the system is about to collapse.

A simple radial system serves as the starting point for the rest of the analysis. It is given by figure 2.7 where the load at bus 2 is $P_L + jQ_L$ and the voltage magnitude is V. The equivalent load admittance is $G_L - jB_L$, where:

$$G_L = \frac{P_L}{V^2}, \qquad B_L = \frac{Q_L}{V^2} \tag{2.23}$$

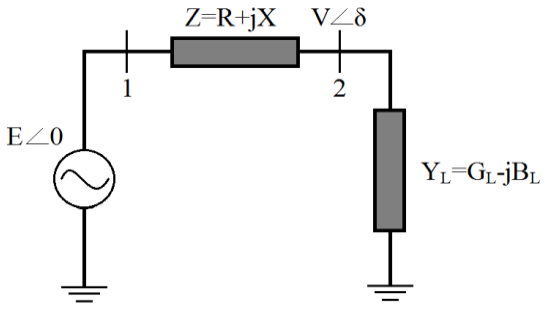

Figure 2.7

Two-bus system to explain the P-index principle

Increasing the network load $P_L + \Delta P_L$ and $Q_L + \Delta Q_L$ while keeping the power factor constant results in a change in load admittance of $G_L + \Delta G_L$ and $B_L + \Delta B_L$. The voltage will drop by V as the load increases. If active power changes, then the change is stated as follows:

$$\begin{aligned} \Delta P_L &= (V + \Delta V)^2 (G_L + \Delta G_L) - V^2 G_L \\ &= (V + \Delta V)^2 \Delta G_L + (2V + \Delta V) G_L \Delta V \end{aligned} \tag{2.24}$$

Two opposing terms combine to form net power. For example, in equation (2.24), the positive term in $(V + \Delta V)^2 \Delta G_L$ indicates the power obtained by increasing ΔG_L, whereas the negative term in $(2V + \Delta V) G_L \Delta V$ represents the power lost by decreasing G_L due to a voltage drop ΔV. The two opposing terms cancel each other out at maximum net power delivered to the load bus.

The P index is based on the fact that the two terms in equation (2.24) tend to be close to each other at the maximum power point; it is based on the ratio of the two terms. The negative sign is used to make the index positive when there is a negative voltage drop for positive ΔG_L:

$$P_{index} = -\frac{(2V + \Delta V) G_L}{(V + \Delta V)^2} \cdot \frac{\Delta V}{\Delta G_L} \tag{2.25}$$

It is possible to express the P-index equation (2.25) as follows when $\Delta G_L,\ \Delta V \ \rightarrow 0$:

$$P_{index} = -\frac{2G_L}{V} \cdot \frac{dV}{dG_L} \tag{2.26}$$

The term $\frac{dV}{dG_L}$ can be expressed in more common terms in the network as follows:

$$\frac{dV}{dG_L} = \frac{dV}{dP_L} \cdot \frac{dP_L}{dG_L} \tag{2.27}$$

From equation (2.23) it can be stated that:

$$dP_L = V^2 dG_L + 2V G_L dV \tag{2.28}$$

Or:

$$\frac{dP_L}{dG_L} = V^2 + 2VG_L\frac{dV}{dG_L} \tag{2.29}$$

Substituting in (2.27):

$$\frac{dV}{dG_L} = \frac{dV}{dP_L}\left(V^2 + 2VG_L\frac{dV}{dG_L}\right) \tag{2.30}$$

Equation (2.30) can be expressed in a different format:

$$\frac{dV}{dG_L} = \frac{V^2\frac{dV}{dP_L}}{1 - 2VG_L\frac{dV}{dP_L}} \tag{2.31}$$

Substituting (2.31) in the P-index formula:

$$P_{index} = \frac{-2VG_L\frac{dV}{dP_L}}{1 - 2VG_L\frac{dV}{dP_L}} \tag{2.32}$$

In terms of active power, the P-index formula can be stated as follows using (2.26):

$$P_{index} = \frac{-2\frac{P_L}{V}\frac{dV}{dP_L}}{1 - 2\frac{P_L}{V}\frac{dV}{dP_L}} \tag{2.33}$$

When normalized voltage and power sensitivity are used, this index provides a more accurate picture of overall system stability than other indices. It is very simple to use, with a value range of 0 for no-load to 1 at the point of collapse.

2.5 Distance to Voltage Collapse using the P-index (The Improved Model)

In [18], an improved estimation for the collapse point calculations was derived. Considering the two bus system in figure 2.7 and assuming the term $\frac{dV}{dG_L}$ remains constant, the voltage magnitude is derived and has the following expression:

$$V = \frac{a}{\sqrt{1 + bG_L + cG_L^2}} \tag{2.34}$$

This equation was derived rigorously starting from the circuit of figure 2.7 with the line resistor $R = 0$, and the load admittance $G - jB$ written as $G(1 - jtan\emptyset)$, where $cos\emptyset$ is the power factor of the load. Solving for the magnitude of the voltage gives:

$$a = E$$

$$b = 2X \cdot tan\phi$$

$$c = X^2(1 + tan^2\phi)$$

The term $\frac{dV}{dG_L}$ can be calculated by taking the derivative of equation 2.34 with respect to G_L. This results in the following:

$$\frac{dV}{dG_L} = \frac{-a(b + 2cG_L)}{2(1 + bG_L + cG_L^2)\sqrt{1 + bG_L + cG_L^2}} = \frac{-a(b + 2cG_L)}{2(1 + bG_L + cG_L^2)^{\frac{3}{2}}} \tag{2.35}$$

Voltage and load conductance can be calculated by using Equation (2.34) and P-index Equation (2.26) at the point of collapse (V_m and G_{Lm}). At the point of collapse, the P-index equals 1. Then:

$$\frac{dV}{dG_L} = \frac{-a(b + 2cG_{Lm})}{2(1 + bG_{Lm} + cG_{Lm}^2)^{\frac{3}{2}}} = -\frac{V_m}{2G_{Lm}} \tag{2.36}$$

Substituting V from (2.34) into (2.36) gives

$$\frac{-a(b + 2cG_{Lm})}{2\sqrt{1 + bG_{Lm} + cG_{Lm}^2}(1 + bG_{Lm} + cG_{Lm}^2)} = \frac{a}{2G_{Lm}\sqrt{1 + bG_{Lm} + cG_{Lm}^2}} \tag{2.37}$$

Solving (2.37) for G_{Lm}:

$$G_{Lm} = \frac{1}{\sqrt{c}} \tag{2.38}$$

The next step is to find the voltage at the maximum loading point by substituting equation (2.38) in equation (2.34). Then, the active power loading at that point becomes:

$$P_m = V_m^2 G_{Lm} \tag{2.39}$$

Or, in terms of loading multiplier λ_m:

$$\lambda_m = \frac{V_m^2 G_{Lm}}{P_0} \tag{2.40}$$

2.5.1 Calculating the constants, a, b, and c

Voltage instability is indicated by an alarm when the most critical node's Pindex value reaches 0.5. This value was proposed in [16] and deemed worthy as an indicator. At this point the constants, a, b, and c may be calculated using the following method;

The coefficient $'a'$ is approximated by setting it to the voltage at no-load condition. This voltage is derived from the following system admittance equation by setting $I_L = 0$.

$$\begin{bmatrix} -I_L \\ I_G \end{bmatrix} = [Y] \begin{bmatrix} V_L \\ V_G \end{bmatrix} = \begin{bmatrix} Y_{LL} & Y_{LG} \\ Y_{GL} & Y_{GG} \end{bmatrix} \begin{bmatrix} V_L \\ V_G \end{bmatrix} \tag{2.41}$$

Solving equation (2.41) for $V_{L0} = V_L|_{I_L=0}$:

$$V_{L0} = -Y_{LL}^{-1} * Y_{LG} * V_G \tag{2.42}$$

Now there is two unknowns left: b and c. These unknowns can only be found using two system equations. $\frac{dV}{dG_L}$ is computed at P-index = 0.5 in equation (2.35):

$$\left.\frac{dV}{dG_L}\right|_{P_{index}=0.5} = \frac{-a(b + 2cG_{L0.5})}{2(1 + bG_{L0.5} + cG_{L0.5}^2)^{\frac{3}{2}}} \tag{2.43}$$

The second system equation is obtained by substituting the voltage (V) and load conductance (G_L) measured at Pindex = 0.5, as well as $a = V_0$, from equation (2.34):

$$V_{0.5} = \frac{a}{\sqrt{1 + bG_{L05} + cG_{L0.5}^2}} \tag{2.42}$$

Solving equations (2.43) and (2.44) to find b and c yield:

$$b = \frac{2a^2}{V_{0.5}^3}\frac{dV}{dG_L} - \frac{2(V_{0.5}^2 - a^2)}{G_{L0.5}^2 V_{0.5}^3} \tag{2.45}$$

And:

$$c = \frac{V_{0.5}^3 - V_{0.5}a^2 - G_{L0.5}a^2\frac{dV}{dG_L}}{G_{L0.5}^2 V_{0.5}^3} \tag{2.46}$$

CHAPTER 3

METHODOLOGY

3.1 Introduction

In this section, three bus indicators have been studied, the L-index, the coupled-single port method, and the P-index. It was attempted to identify factors that would probably cause inaccurate behavior, such are mis-ranking and overestimation in the case of the L-index/coupled port, or mis-ranking in the case of the P-index. In the case of the L-index/coupled port, the main deficiency results from incomplete model information, in particular the generator currents. It was shown that an attempt to account for generator voltage variation would reflect on the 'no-load voltage' $\underline{V_{0j}}$ of equation (2.10). This voltage is considered constant in the main derivation for the aforementioned indicators, and this is not the case in reality. The P-index is examined also as mentioned, and it was found that it is not always able to pick the best bus for estimation of the voltage collapse, which may not necessarily coincide with the highest P-index bus. Since estimation is based on an emulation of a two-bus system, it is postulated that a good choice would be a bus that exhibits the most radial behavior, i.e. a bus that has the highest impedance to source as measured from the Z_{LL} matrix of equation (2.7). At the same time, P-index ranking is important, so we devise what we term as 'bus participation' in the collapse, which is essentially the P-index of all buses weighted by their relative radial behavior, taking the elements of Z_{LL} as weights. the weighted P-index

method was tested on benchmark systems, and it was observed that it leads to improving bus rankings and consequently improving estimation of the collapse point in many cases.

Before proceeding we need to mention that the coupled single-port method is only a slightly different reformulation of the L-index approach. Recall that the L-index was described as calculated by the expression in equation (2.12)

$$L_j = \left| \frac{\sum_{i \in L} \underline{Z}_{ji} \cdot \underline{I}_j}{\underline{V}_j} \right| \tag{3.1}$$

Compare this to the criteria in the Coupled-Single-Port Circuit (CSPC) for maximum power that can be delivered to the measurement point can be calculated using matching impedance condition $|Z_{load}| = |Z_{line}|$. For a radial circuit, this leads to the bus voltage magnitude $\left|\underline{V}_{load}\right| = \left|\underline{Z}_{load} \times \underline{I}_{load}\right|$ being equal to line voltage drop $\left|\underline{Z}_{line} \times \underline{I}_{load}\right|$. From the model of the CSPC method equation (2.17), the total voltage drop on the line $= \underline{Z}_{eqj}\underline{I}_{Lj} + \underline{E}_{coupled-j}$, where

$\underline{Z}_{eqj} = \underline{Z}_{LLjj}$ and $\underline{E}_{coupled-j} = \sum_{i \neq j; i=1}^{n_L} \underline{Z}_{LLji}\underline{I}_{Li}$. They model this $\underline{E}_{coupled-j}$ as an additional impedance, giving a total $\underline{Z}_{line} = \underline{Z}_{LLjj} + \frac{\sum_{i \neq j; i=1}^{n_L} \underline{Z}_{LLji}\underline{I}_{Li}}{\underline{I}_{Lj}}$. The total voltage drop along the line is then $\underline{Z}_{LLjj} + \sum_{i \neq j; i=1}^{n_L} \underline{Z}_{LLji}\underline{I}_{Li}$. But the sum of these two terms is just $\sum_{i=1}^{n_L} \underline{Z}_{LLji}\underline{I}_{Li}$. Thus the condition for maximum power transfer ($\left|\underline{V}_{load}\right| = \left|\underline{Z}_{line} \times \underline{I}_{load}\right|$) is actually

$$\left|\underline{V}_j\right| = \left| \sum_{i=1}^{n_L} \underline{Z}_{LLji}\underline{I}_{Li} \right| \tag{3.2}$$

Or,

$$1 = \left| \frac{\sum_{i=1}^{n_L} \underline{Z}_{LLji} \underline{I}_{Li}}{\underline{V}_j} \right| \tag{3.3}$$

Which is exactly the same criteria of the L-index at maximum power transfer. The conclusion is that the Coupled-Single-Port Circuit method, although formulated differently, offers the same estimation as the L-index, and therefore does not realize an improvement in this regard. The method does introduce the use of the formulation for S_{max} in equation (2.21), something not included in the original L-index paper.

For testing the accuracy of the L-index (and by extension the CSPC) method, there is a need for a benchmark point for measurement. Since an agreed point of alarm is lacking in the L-index and CSPC method, the alarm criteria defined in the P-index method was used, which defines the alarm at $\frac{P}{V}\frac{dV}{dP} = 0.5$. This unified criterion further helps in gauging the accuracy across different methods.

The testing will proceed as follows: select a particular system and perform any required outage. Carry out continuation power flows, increasing the loading parameter λ until one of the buses reaches $\frac{P_j}{V_j}\frac{dV_j}{dP_j} = 0.5$. This is the selected bus for estimation. Calculate the network Z_{LL} according to equation (2.7) and the equivalent $\underline{Z}_{eq} = \frac{\sum_{i \in L} \underline{Z}_{ji} \cdot \underline{I}_i}{\underline{I}_j}$ as defined by either the L-index or the CSPC methods. Find also $\underline{E}_{eqj} = \left[K\underline{V}_G\right]_j$ and finally substitute in equation (2.21) to find S_{max} with knowledge of load power factor. Compare the accuracy of the estimated S_{max} against the actual S_{max} obtained from a continuation power flow or repeated load flows. Tabulate the results and display graphically for different network outages. The novelty in this approach is using a unified gauge for comparison.

To test the revised indicated of the P-index when weighted by the Z_{LL} matrix of (2.7), a particular system was selected and then performed any required outage. Then carry out continuation power flows, and increase the loading parameter λ until one of the buses reaches $\frac{P_j}{V_j}\frac{dV_j}{dP_j} = 0.5$. At this point, the P-index for all load buses was found, including the one with the highest P-index of 0.5. At the same time, the Z_{LL} matrix was computed. The weighted P-index for bus j is then found as follows,

$$Pindex\_j\_w = \frac{\sum_{i=1}^{Nload} Pindex\_i \times Z_{LLji}}{\sum_{i=1}^{Nload} Z_{LLji}} \tag{3.4}$$

Where $Nload$ is the number of load buses.

If the load bus j is representative of a highly radial feeder load point, then its self-impedance to source Z_{LLjj} will be much larger than other (mutual) impedances Z_{LLji} (or $Z_{LLjj} \gg Z_{LLji}$). In this case the weighted P-index will be largely equal to the original P-index ($Pindex\_j\_w \approx Pindex\_j$), and its ranking in relation to other buses would not be affected. However, if the feeder of bus j has a high portion of distributed loads, then it is postulated that the estimation to collapse associated with this feeder will not give good results when using equation (2.34), which was derived around radial feeders. The weighted $Pindex\_j\_w$ rank will be demoted depending on the different weights, and another bus k that has a higher radial property ($Z_{LLkk} \gg Z_{LLki}$) may be promoted as the best bus for estimation, even if it has a slightly lower $Pindex\_k$ compared to $Pindex\_j$.

Having selected the buses using these criteria, estimation to collapse is made and compared with the estimation to collapse using the original method (bus with highest P-index) to see if it offers better results.

CHAPTER 4

RESULTS AND DISCUSSION

A MATLAB prototype for the proposed methods of qualitative analysis was written to compare the estimated voltage collapse against actual collapse point for the two different approaches on the IEEE 14, 57, and 118-bus systems. Selected outages were performed, and comparative results for L-index and bus participation methods were procured for these outages. The following sections present a thorough illustration of the proposed approaches.

4.1 Examining the L-index results on the IEEE 14, 57, and 118-Bus Systems

The L-index comparisons were tested on all possible outages of the IEEE-14 bus system shown in Figure 4.1, and selected outages on the IEEE-57 (Figure 4.3) and IEEE-118 (Figure 4.5) buses. The load multiplier was gradually increased, and max value was calculated for each mode.

The estimation error was displayed graphically against the L-index measured at the alarm point $\left(\frac{P_j}{V_j}\frac{dV_j}{dP_j} = 0.5\right)$, Figures 4.2, 4.4, and 4.6. The general observation which was especially true for the IEEE-14 and IEEE-118 systems was that when the value of the L-index was low, giving the impression the system was far from the point of collapse, the reality was that the collapse point was much closer, and there was a gross over-estimation of distance to collapse. Additionally, the lower the L-index the larger the error as is observed from the graph for these two systems.

Another observation was that the estimations for IEEE-57 were lower than the actual point of collapse, i.e. overly pessimistic. This leads to speculation about the nature of the system, and it

is observed to have sparse generation, leading to high values of the Z_{LL} matrix elements. Indeed, when looking at similar cases in the IEEE-14, and IEEE-118 bus systems underestimations occur in the regions further away from generation, or when an outage results in a radial feeder.

Conversely, the worst results, which were the mentioned overestimations in the IEEE-14, and IEEE-118 would happen when the outage does not result in a radial feeder, particularly in heavy generator populated areas. The absolute worst case is an outage between two generators or an outage that does not result in a radial network, such as network splits. The vulnerability in this case that the L-index seems unable to capture is due to increase power transfers between generation centers, as opposed to the classical power transfer between generator and load.

4.1.1 IEEE 14-bus System

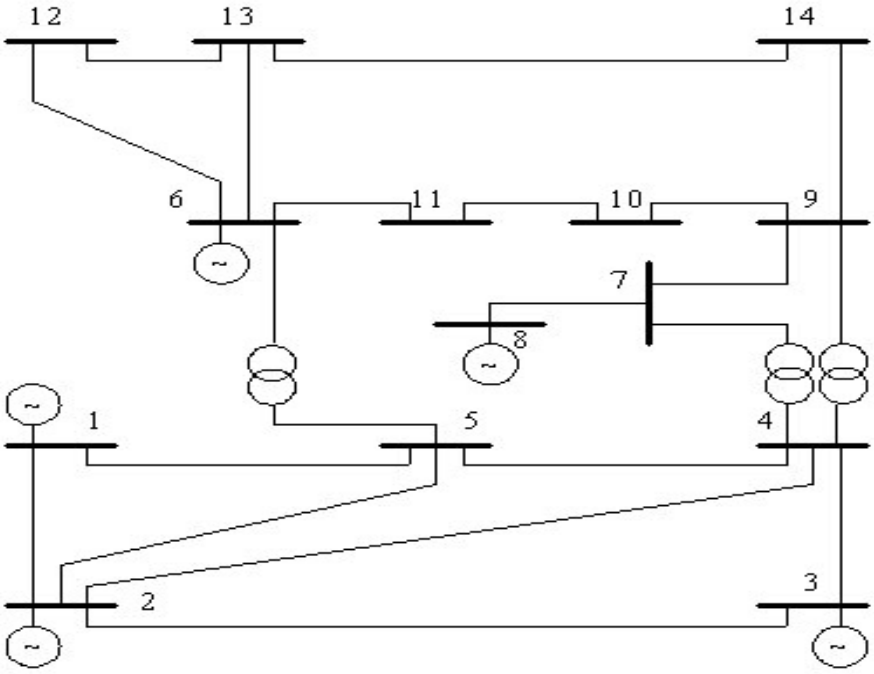

Figure 4.1

Single-Line Diagram of IEEE 14-Bus System

Table 4.1

Estimation of Collapse Point Based on L-index, IEEE 14-bus System

Estimation Carried out at $\left(\frac{P_j}{V_j}\frac{dV_j}{dP_j} = 0.5\right)$

Case	**λ alarm**	**L-index**			**Actual λmax**	**Error (%)**
		Bus	**Index**	**Estimated λmax**		
Intact	3.35	14	0.37	4.47	4.04	-10.6
1-2 out	1.29	14	0.1	4.26	1.34	-217
1-5 out	3.1	14	0.33	4.37	3.66	-19.3
2-3 out	2.09	14	0.19	4.26	2.27	-87.6
2-4 out	2.78	14	0.29	4.25	3.29	-29.1
2-5 out	2.88	14	0.30	4.35	3.43	-26.8
3-4 out	3.29	14	0.37	4.38	3.94	-11.1
4-5 out	3.24	14	0.39	4.2	3.94	-6.5
4-7 out	3.01	14	0.34	4.19	3.6	-16.3
4-9 out	3.23	14	0.39	4.19	3.94	-6.3
5-6 out	2.1	14	0.19	4.32	2.28	-89.4
6-11 out	2.58	11	0.41	3.3	3.53	6.9
6-12 out	3.21	14	0.38	4.2	3.98	-5.5
6-13 out	2.39	14	0.41	3	3.22	6.8
7-9 out	2.2	9	0.39	2.82	2.87	1.7
9-10 out	3.25	14	0.36	4.41	4	-10.2
9-14 out	2.81	14	0.41	3.5	3.7	5.4
10-11 out	2.84	10	0.38	3.77	3.73	-1.07
12-13 out	3.31	14	0.33	4.38	4.02	-8.95
13-14 out	2.38	14	0.43	2.95	3.24	8.9

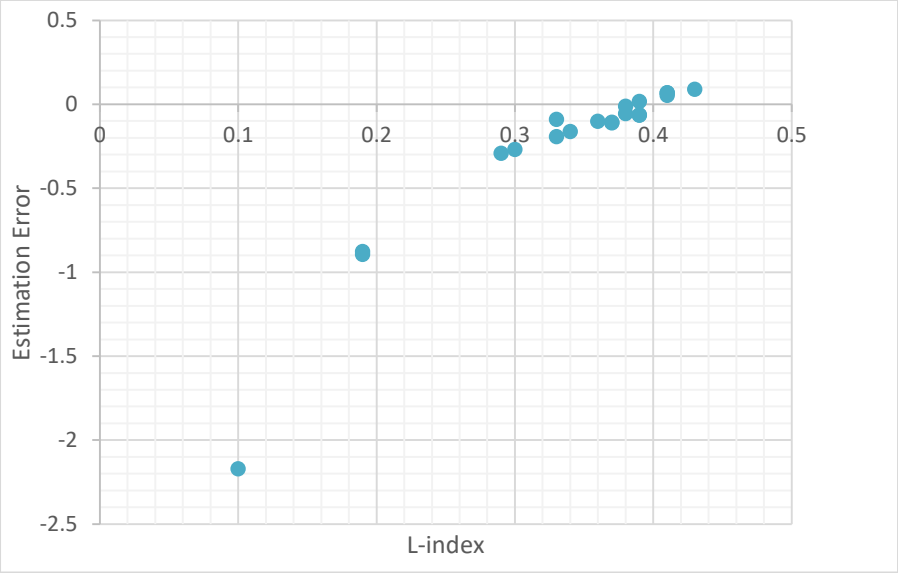

Figure 4.2

Estimation Error against L-index for all possible outages of the IEEE 14-bus system

4.1.2 IEEE 57-bus System

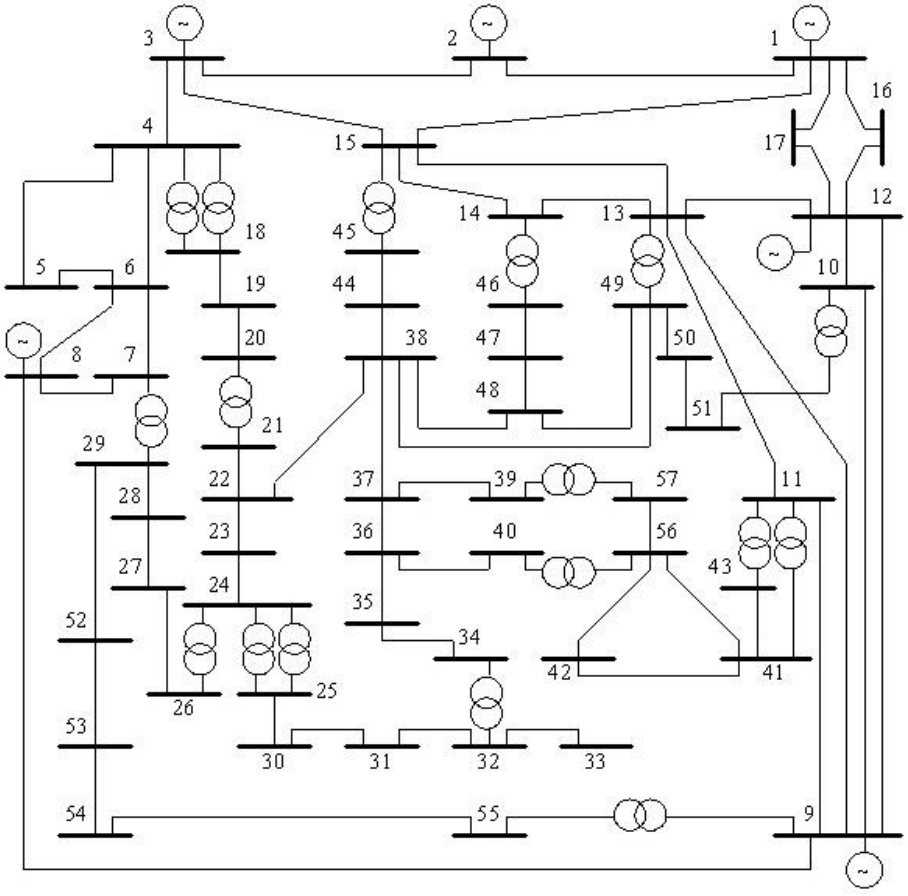

Figure 4.3

Single Line Diagram of the IEEE 57-Bus System

Table 4.2

Estimation of Collapse Point Based on L-index, IEEE 57-bus System

Estimation Carried out at $\left(\frac{P_j}{V_j}\frac{dV_j}{dP_j} = 0.5\right)$

Case	**λ**	**L-index**			**Actual λ**	**Error (%)**
		Bus	**Index**	**λ Estimated**		
Intact	1.3	31	0.4912	1.5178	1.85	17.95
4-5 out	1.3	31	0.4914	1.5175	1.85	17.97
1-15 out	1.27	31	0.4961	1.4766	1.81	18.41
13-14 out	1.28	31	0.4915	1.4942	1.82	17.90
7-29 out	1	29	0.6506	1.0556	1.14	7.4
23-24 out	1.2	31	0.4780	1.4146	1.68	15.79
24-25 out	1.12	31	0.4917	1.3095	1.55	15.51
24-26 out	1.15	31	0.4778	1.3559	1.64	17.32
22-38 out	1.16	31	0.4842	1.3612	1.64	17
37-38 out	1	33	0.6856	1.0454	1.18	11.40

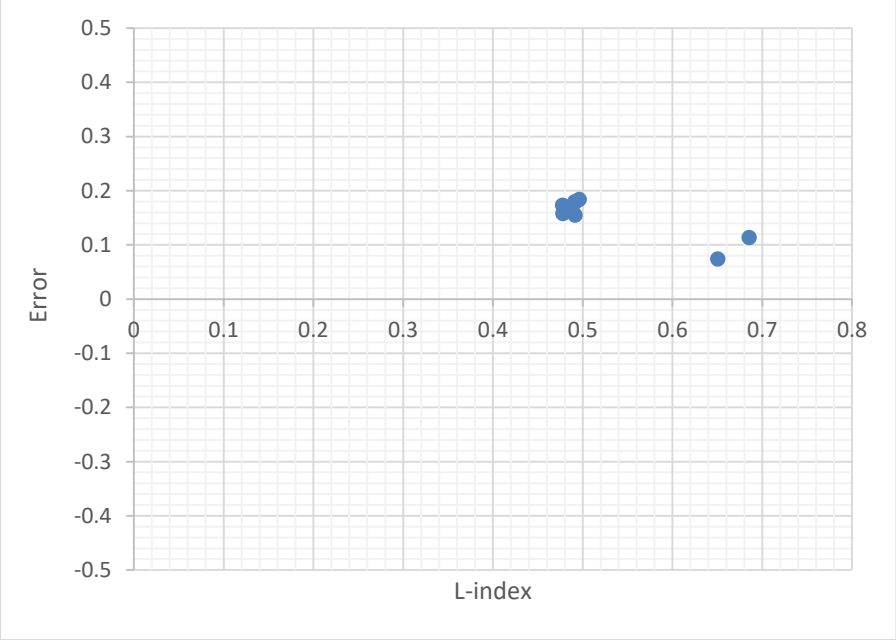

Figure 4.4

Estimation Error against L-index for some outages of the IEEE 57-bus System

4.1.3 IEEE 118-bus System

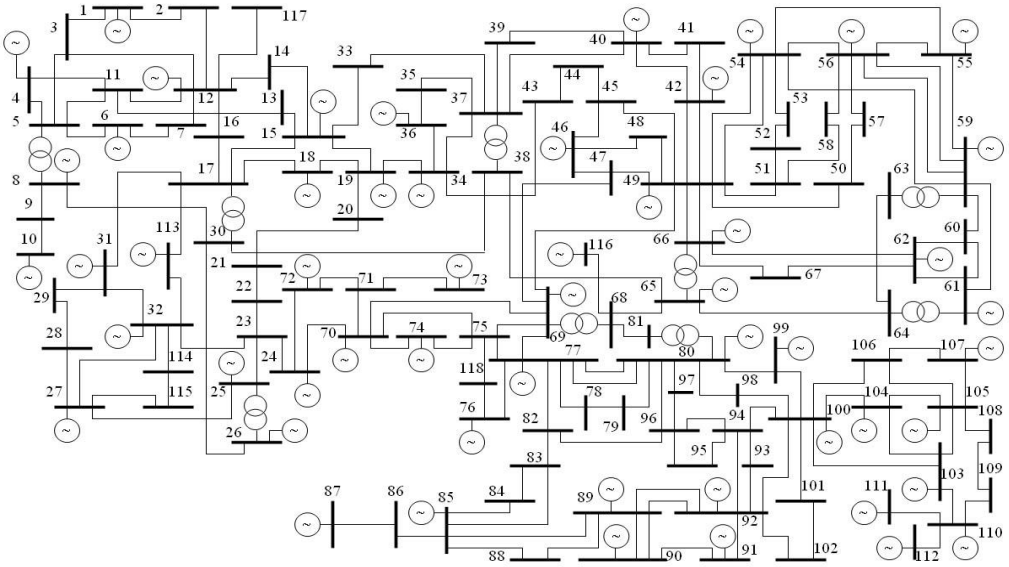

Figure 4.5

Single Line Diagram of the IEEE 118-Bus System

Table 4.3

Estimation of Collapse Point Based on L-index, IEEE 118-bus System Estimation Carried out at $\left(\frac{P_j}{V_j}\frac{dV_j}{dP_j} = 0.5\right)$

Case	**λ**	**L-index**			**Actual λ**	**Error (%)**
		Bus	**Index**	**λ Estimated**		
Intact	2.78	44	0.26	4.54	3.19	-42.49
11-13 out	2.33	13	0.40	2.96	2.96	-0.17
19-20 out	2.05	20	0.43	2.56	2.64	2.92
23-24 out	2.64	44	0.24	4.52	2.97	-52.18
23-25 out	2.71	44	0.25	4.58	3.08	-48.73
26-30 out	2.09	44	0.17	4.56	2.6	-75.68
44-45 out	2.41	44	0.44	2.94	2.98	1.08
75-77 out	2.76	44	0.26	4.52	3.17	-42.80
77-78 out	2.52	78	0.42	3.14	3.19	1.58

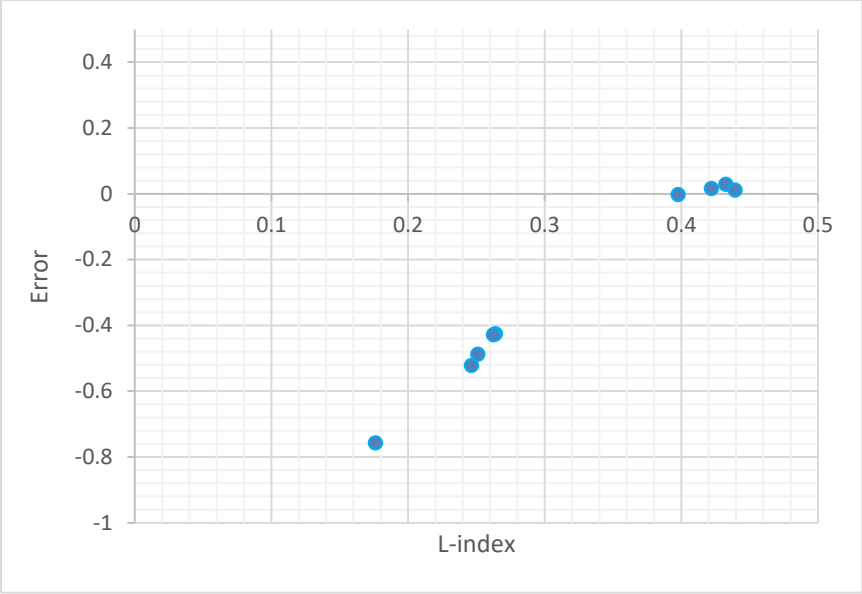

Figure 4.6

Estimation Error against L-index for some outages of the IEEE 118-bus System

4.2 Redefining the P-index to account for bus participation and testing the result on the IEEE 14, 57, and 118-Bus Systems

As described in Chapter 3, an attempt to redefine the P-index was performed, such that it does not necessarily select the bus with the highest P-index for estimation of distance to collapse, but rather a bus with both highest P-weighted by the *radial* characteristics of the bus. It was gauged how radial a bus is by looking at its corresponding row in the Z_{LL} matrix, and consider the weight of the self-impedance Z_{LLjj} in relation to the mutuals Z_{LLji} (even though we recognize that this approach may not capture cases involving generator or network splitting as per previous discussion on the L-index). Thus, after selecting an outage, power flows were performed with increasing λ until one of the buses hits $\frac{P_j}{V_j}\frac{dV_j}{dP_j} = 0.5$. Then carry out the following exercise to find the weighted P-index for bus j,

$$Pindex\_j\_w = \frac{\sum_{i=1}^{Nload} Pindex\_i \times Z_{LLji}}{\sum_{i=1}^{Nload} Z_{LLji}}$$

4.2.1 IEEE 14-bus System

Table 4.4

Comparison between P-index Bus Participation Method and (a = V_0 Method) for IEEE 14-bus System

Case	λ_m (Actual)	$a = V0$ Method			P-index Bus Participation Method		
		Critical Bus	λ_m	Error (%)	Critical Bus	λ_m	Error (%)
Intact	4.04	14	4.21	-4.30	5	4.01	0.59
1-2 Out	1.34	5	1.43	-7.07	5	1.43	-7.07
1-5 Out	3.65	5	3.65	0.05	5	3.65	0.05
2-3 Out	2.26	4	2.39	-5.60	5	2.43	-7.31
2-4 Out	3.29	5	3.26	0.85	5	3.26	0.85
2-5 Out	3.43	5	3.38	1.34	5	3.38	1.34
3-4 Out	3.94	14	4.12	-4.51	5	3.97	-0.8
4-5 Out	3.94	14	4.12	-4.64	5	3.97	-0.8
4-7 Out	3.60	14	3.77	-4.66	5	3.66	-1.77
4-9 Out	3.94	14	4.08	-3.55	14	4.08	-3.55
5-6 Out	2.28	14	2.44	-6.87	14	2.44	-6.87
6-11 Out	3.52	11	3.29	6.54	11	3.29	6.54
6-12 Out	3.98	14	4.06	-2.13	14	4.06	-2.13
6-13 Out	3.22	14	3.10	3.59	13	3.14	2.41
7-9 Out	2.87	9	2.79	2.85	9	2.79	2.85
9-10 Out	4.00	14	4.07	-1.54	14	4.07	-1.54
9-14 Out	3.70	14	3.67	0.62	14	3.68	0.62
10-11 Out	3.73	10	3.55	4.84	10	3.55	4.84
12-13 Out	4.02	14	4.16	-3.27	14	4.16	-3.27
13-14 Out	3.24	14	3.07	5.36	14	3.07	5.36

4.2.2 IEEE 57-bus System

Table 4.5

Comparison between P-index Bus Participation Method and (a = V_0 Method) for IEEE 57-bus System

Case	λ_m (Actual)	$a = V0$ Method			P-index Bus Participation Method		
		Critical Bus	λ_m	Error (%)	Critical Bus	λ_m	Error (%)
Intact	1.84	31	1.7404	5.41	31	1.7404	5.41
1-15 out	1.8	31	1.7073	5.15	31	1.7073	5.15
7-29 out	1.13	29	1.1181	1.053	53	1.1370	-0.61
13-14 out	1.81	31	1.7139	5.30	31	1.7139	5.30
22-38 out	1.63	31	1.5559	4.54	31	1.5559	4.54
23-24 out	1.67	31	1.604	3.95	31	1.604	3.95
24-26 out	1.63	31	1.5505	4.87	31	1.5505	4.87
37-38 out	1.17	33	1.1442	2.20	31	1.1693	0.059

4.2.3 IEEE 118-bus System

Table 4.6

Comparison between P-index Bus Participation Method and (a = V $_0$ Method) for IEEE 118-bus System

Case	λ_m (Actual)	$a = V0$ Method			P-index Bus Participation Method		
		Critical Bus	λ_m	Error (%)	Critical Bus	λ_m	Error (%)
Intact	3.18	44	3.34	-5.15	44	3.34	-5.15
11-13 out	2.95	13	2.95	-0.08	13	2.95	-0.08
19-20 out	2.63	20	2.56	2.657	20	2.56	2.65
23-24 out	2.97	44	3.15	-6.21	44	3.15	-6.21
23-25 out	3.07	44	3.27	-6.51	44	3.27	-6.51
26-30 out	2.60	22	2.49	3.873	22	2.49	3.87
44-45 out	2.97	44	3.11	-4.67	44	3.11	-4.67
75-77 out	3.17	44	3.33	-5.09	44	3.33	-5.09
77-78 out	3.18	78	3.20	-0.75	78	3.20	-0.75

The P-index is a much more successful indicator compared to the L-index. In all studies performed, it rarely offered an error of more than 6% in distance to collapse. This also provides good justification for using its key term $\frac{P_j}{V_j}\frac{dV_j}{dP_j}$ as an alarm indicator $\left(\frac{P_j}{V_j}\frac{dV_j}{dP_j} = 0.5\right)$. After redefining the P-index as described and testing it on our benchmark systems, the results show that it was successful in improving many cases through selecting alternative buses for estimation. Only one case gave a worse result, namely the case of the inter-generator link outage 2-3 on the IEEE-14-bus system. The cases for which an improvement in estimation was realized are highlighted in cyan, those for which a drop in accuracy happened are highlighted in yellow. All other cases (where the estimating bus did not change) are left un-highlighted.

looking at cases where a change in bus was determined, such as the intact IEEE-14 system, it can be seen that a change from bus 14 to bus 5 was made. Closer analysis reveals that bus 5 although having a lower P-index than bus 14 it enjoys slightly greater participation in the collapse compared to the latter. The weighted product of the $\frac{Pindex\_i \times Z_{LLji}}{\sum Z_{LLji}}$ is shown in Table 4.7. it can be seen that the resulting weighted P-index ($Pindex\_j\_w$) for bus 5 is dominated by the weights of bus 4 and 5, while the weighted P-index for bus 14 is spread over the weights of bus 9 to 14 (which heavy emphasis on bus 14). Bus 5 wins because together with bus 4 it outweighs the participation of bus 14 and its neighbors.

Table 4.7

The weighted product of the $\frac{Pindex\_i \times Z_{LLji}}{\sum Z_{LLji}}$

	Bus 4	Bus 5	Bus 7	Bus 9	Bus 10	Bus 11	Bus 12	Bus 13	Bus 14	**Sum**
Bus 5	0.103	0.1768	0	0.0472	0.0369	0.0129	0.0009	0.0034	0.0300	**0.4105**
Bus 14	0.0102	0.0065	0	0.0647	0.0512	0.0173	0.0081	0.0238	0.2202	**0.4017**

The inability of the Z_{LL} approach to capture network splitting and outages involving links between generators is again seen here. The outage of line 2-3 between generators 2 and 3 results in selection of a new bus which yield a declining accuracy. It is also observed that the case of outage 1-2 fails to shift from bus 5 to bus 4, which would have yielded a better result outcome. Clearly, this is an issue that needs further investigation.

CHAPTER 5

CONCLUSION AND FUTURE WORK

5.1 Conclusion

The reviewed indicators show that estimation to collapse depends on how radial the bus used for estimation is with respect to the system. The general observation was that a bus that is in close proximity (electrically) to generators that are tightly coupled would tend to overestimate the point of collapse, whereas buses remote from generators would tend to underestimate. Strictly radial feeders with few distributed loads along the way seem to give good results such as bus 14 on an outage of 9-14 of the IEEE 14-bus system or bus 13 in the outage of 11-13 in the IEEE 118-bus system, but more evidence is required to support this.

Gross overestimation in the L-index is observed with the outage of inter-generator lines or lines that couple generator centers – the P-index also shows overestimation in this case albeit with much less error. It would seem that the Z_{LL} bus method which uses elements of Z_{LLji} to model the radial feeder for bus j and V_{0j} to model the Thevenin voltage is not a good model for such cases. There is some evidence that more impedance behind V_{0j} exists, and indeed a recent paper [19] attempts to calculate such an impedance. Treating V_{0j} as a constant Thevenin voltage composed of all generators and synchronous condensers in a power system is clearly an approximation on many levels. First, the angle of the generator's changes with the loading parameter λ as the load grows, and second, the active power generation is fixed for the generators (and tied to λ), whereas

in a true Thevenin source no such limitation would exist. Future research would do good to focus on finding a convenient way of identifying the behavior behind V_{0j}.

5.2 Future work

This work has shown that there is some benefit in identifying bus participation in the collapse by weighting the P-index, but that using the Z_{LL} bus matrix could be marred by the same flaws discussed in the previous section. Therefore, some alternative or strengthened weighting is needed, for example by exploring the additional impedances talked about in the context of the L-index. Another idea would be to use modal analysis, which in other stability contexts has shown success in identifying mode participation.

REFERENCES

[1] G. M. Huang and L. Zhao, "Measurement based voltage stability monitoring of power system," *Power Syst. Eng. Res. Ctr,* 2001.

[2] P. Kundur, "Power Systems Stability and Control. New York, McGraw-Hi1l," in *Conference Proceedings*, 1994.

[3] M. Kamel, "Development and application of a new voltage stability index for on-line monitoring and shedding," 2016.

[4] C. E. Doig Cardet, "Analysis on voltage stability indices," 2010.

[5] P.-A. Lof, T. Smed, G. Andersson, and D. Hill, "Fast calculation of a voltage stability index," *IEEE Transactions on Power Systems,* vol. 7, no. 1, pp. 54-64, 1992.

[6] J. Van Hecke, N. Hatziargyriou, and T. Van Cutsem, "Indices predicting voltage collapse including dynamic phenomena," *Report of CIGRE working group 38.02. 11,* p. 94, 1994.

[7] H.-D. Chiang and R. Jean-Jumeau, "Toward a practical performance index for predicting voltage collapse in electric power systems," *IEEE Transactions on power systems,* vol. 10, no. 2, pp. 584-592, 1995.

[8] A. Z. De Souza, C. A. Canizares, and V. H. Quintana, "New techniques to speed up voltage collapse computations using tangent vectors," *IEEE Transactions on Power systems,* vol. 12, no. 3, pp. 1380-1387, 1997.

[9] A. Berizzi, P. Finazzi, D. Dosi, P. Marannino, and S. Corsi, "First and second order methods for voltage collapse assessment and security enhancement," *IEEE Transactions on Power Systems,* vol. 13, no. 2, pp. 543-551, 1998.

[10] M. Moghavvemi and G. Jasmon, "New method for indicating voltage stability condition in power system," in *Proc. Third Int. Power Engineering Conf., Singapore*, 1997, vol. 1, pp. 223-227.

[11] N. Hang, T. Xu, Q. Liao, and Z. Lu, "The analysis of abundance index of voltage stability based circuit theory," *Guangxi Electric Power,* vol. 2, p. 002, 2006.

[12] A. Mohamed, G. Jasmon, and S. Yusoff, "A static voltage collapse indicator using line stability factors," *Journal of industrial technology,* vol. 7, no. 1, pp. 73-85, 1989.

[13] I. Musirin and T. A. Rahman, "Novel fast voltage stability index (FVSI) for voltage stability analysis in power transmission system," in *Student conference on research and development*, 2002: IEEE, pp. 265-268.

[14] M. Moghavvemi and O. Faruque, "Real-time contingency evaluation and ranking technique," *IEE Proceedings-Generation, Transmission and Distribution*, vol. 145, no. 5, pp. 517-524, 1998.

[15] P. Kessel and H. Glavitsch, "Estimating the voltage stability of a power system," *IEEE Transactions on power delivery*, vol. 1, no. 3, pp. 346-354, 1986.

[16] M. Kamel, A. A. Karrar, and A. H. Eltom, "Development and application of a new voltage stability index for on-line monitoring and shedding," *IEEE Transactions on power systems*, vol. 33, no. 2, pp. 1231-1241, 2017.

[17] Y. Wang *et al.*, "Voltage stability monitoring based on the concept of coupled single-port circuit," *IEEE Transactions on Power Systems*, vol. 26, no. 4, pp. 2154-2163, 2011.

[18] S. Mohammed, A. H. Eltom, and A. Karrar, "Improved Computations of the Voltage Collapse Point," in *2019 IEEE Power & Energy Society General Meeting (PESGM)*, 2019: IEEE, pp. 1-5.

[19] P. Ye, X. Han, M. Yang, Y. Zhang, Y. Pei, and X. Zhang, "A Novel Thévenin Equivalent Model Considering the Correlation of Source-Grid-Load in Power Systems," *IEEE Access*, vol. 9, pp. 31276-31286, 2021.

VITA

Mohamed Mohamed was born in Jeddah, Saudi Arabia in 1993 to the parents of Salah and Manal. In 2016, he earned his Bachelor of Science (Honors) in Electrical and Electronic Engineering with First Class at the University of Khartoum, Sudan. After graduation, he worked as an electrical engineer at the Sudanese Electricity Distribution Company (SEDC) until he was awarded a graduate assistantship, in January 2020, from the University of Tennessee at Chattanooga to pursue his master's degree in Electrical Engineering. Currently, Mohamed works for Mesa Associates Inc. in Chattanooga, Tennessee, and he is to graduate in December 2021.